AD-A168 634 IMPROVEMENT OF FRACTURE TOUGHNESS IN HIGH STRENGTH BETA TITANIUM ALLOYS(U) GEORGE WASHINGTON UNIV WASHINGTON DC SCHOOL OF ENGINEERING AN.. P K POULOSE ET AL. 1/1

UNCLASSIFIED 18 MAR 85 N00019-83-C-0177 F/G 11/6 NL

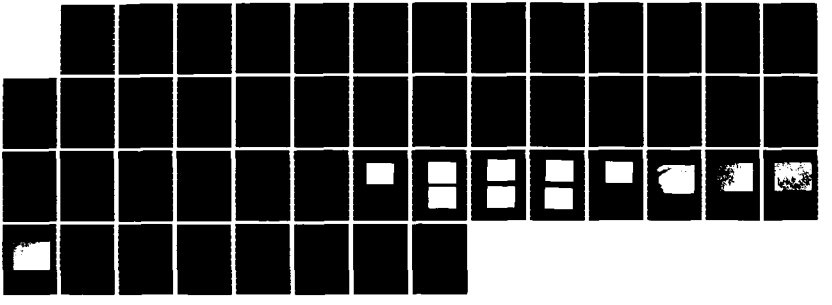

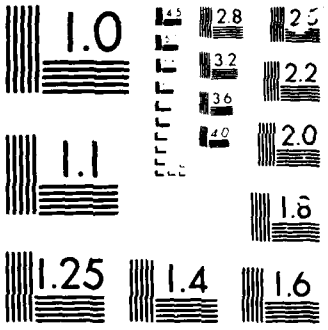
1.0
1.1
1.25
1.4
1.6
2.8
3.2
3.6
4.0
2.2
2.0
1.8

IMPROVEMENT OF FRACTURE TOUGHNESS IN HIGH STRENGTH BETA TITANIUM ALLOYS

P. K. Poulose and H. Liebowitz

NAVAIR Contract No. N00019-83-C-0177

Final Technical Report

Approved for public release; Distribution is unlimited

School of Engineering and Applied Science
The George Washington University
Washington, D.C. 20052

REPORT DOCUMENTATION PAGE

1a REPORT SECURITY CLASSIFICATION Unclassified	1b RESTRICTIVE MARKINGS None
2a SECURITY CLASSIFICATION AUTHORITY N/A	3 DISTRIBUTION/AVAILABILITY OF REPORT Unlimited
2b DECLASSIFICATION/DOWNGRADING SCHEDULE N/A	
4 PERFORMING ORGANIZATION REPORT NUMBER(S) None	5 MONITORING ORGANIZATION REPORT NUMBER(S)
6a NAME OF PERFORMING ORGANIZATION The George Washington University 6b OFFICE SYMBOL (If applicable)	7a NAME OF MONITORING ORGANIZATION Department of the Navy Naval Air Systems Command
6c ADDRESS (City, State, and ZIP Code) School of Engineering and Applied Science Washington, D.C. 20052	7b ADDRESS (City, State, and ZIP Code) Naval Air Systems Command Headquarters Washington, D.C. 20361
8a NAME OF FUNDING/SPONSORING ORGANIZATION Naval Air Systems Command 8b OFFICE SYMBOL (If applicable)	9 PROCUREMENT INSTRUMENT IDENTIFICATION NUMBER Contract N00019-83-C-0177
8c ADDRESS (City, State, and ZIP Code) Naval Air Systems Command Headquarters Washington, D.C. 20361	10 SOURCE OF FUNDING NUMBERS PROGRAM ELEMENT NO / PROJECT NO / TASK NO / WORK UNIT ACCESSION NO

11 TITLE (Include Security Classification)

Improvement of Fracture Toughness in High Strength Beta Titanium Alloys

12 PERSONAL AUTHOR(S)
P. K. Poulose and H. Liebowitz

13a TYPE OF REPORT	13b TIME COVERED	14 DATE OF REPORT (Year, Month, Day)	15 PAGE COUNT
Final Technical Report	FROM 9/30/83 TO 10/29/84	March 18, 1985	47

16 SUPPLEMENTARY NOTATION

Approved for public release; distribution is unlimited

17 COSATI CODES			18 SUBJECT TERMS (Continue on reverse if necessary and identify by block number)
FIELD	GROUP	SUB-GROUP	

19 ABSTRACT (Continue on reverse if necessary and identify by block number)

Specimens of beta titanium alloy, Ti-15-3, were heat treated to different strength levels by single-stage and multi-stage ageing, and hardness, tensile and fracture properties were determined to identify heat treatments well suited for structural applications. These studies were supplemented by microstructural analysis. Attractive combinations of strength and fracture toughness were obtained at medium to high strength levels. The relationship between microstructure and mechanical properties is discussed.

20 DISTRIBUTION/AVAILABILITY OF ABSTRACT ☒ UNCLASSIFIED UNLIMITED ☐ SAME AS RPT ☐ DTIC USERS	21 ABSTRACT SECURITY CLASSIFICATION Unclassified
22a NAME OF RESPONSIBLE INDIVIDUAL Dr. Harold Liebowitz	22b TELEPHONE (Include Area Code) (202) 676-6080 22c OFFICE SYMBOL

DD FORM 1473, 84 MAR 83 APR edition may be used until exhausted
All other editions are obsolete

ABSTRACT

Specimens of beta titanium alloy, Ti-15-3, were heat treated to different strength levels by single-stage and multi-stage ageing, and hardness, tensile and fracture properties were determined to identify heat treatments well suited for structural applications. These studies were supplemented by microstructural analysis. Attractive combinations of strength and fracture toughness were obtained at medium to high strength levels. The relationship between microstructure and mechanical properties is discussed.

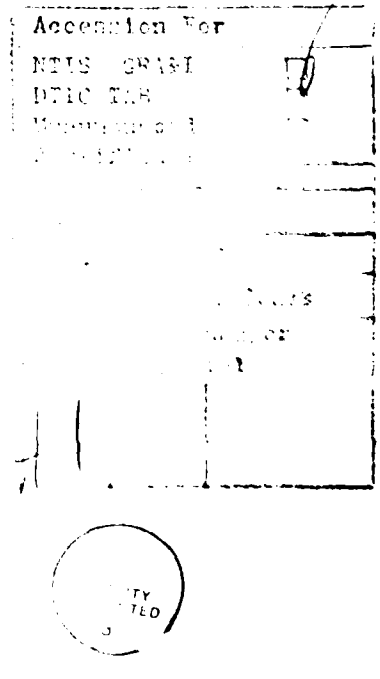

INTRODUCTION

Titanium alloys have come into prominence as aircraft structural materials because of their high strength-to-weight ratio and excellent corrosion resistance. Based on the microstructures that can be produced by alloy additions, titanium alloys are grouped as alpha, alpha-beta and beta alloys. The commercially available structural alloys are mostly alpha-beta alloys, but, recently, there has been considerable interest in beta alloys. Both alpha-beta and beta alloys contain α and β as micro-constituents in the strengthened condition. The strength of these alloys is controlled by the size, shape, distribution and percentage of the α phase. The elastic modulus also increases with α content. The α-β alloys contain more than one phase at room temperature. If cooling after high temperature treatment is slow α precipitates from the β phase, and faster cooling from high temperature produces martensite in the beta matrix. On the other hand, in beta alloys, the metastable β phase can be retained at room temperature without decomposition, by fast cooling after high temperature thermomechanical treatments.

The slow rate of transformation from beta can be effectively made use of for mechanical processing and control of strength and fracture toughness of these alloys. A major disadvantage of the alpha-beta alloys is

that their poor cold formability, due to the invariable presence of the hexagonal phase α or α' at low temperatures limiting the ductility. Compared to this, the beta alloys can be obtained as single phase ß at room temperature. The beta phase is body centered cubic in structure, and is ductile. Its cold formability is very good. The beta alloys can be formed into thin sheets and strips [1]. After forming operations the beta alloys can be heat treated later to the desired strength and toughness levels. The beta alloys are also more amenable to high temperature processing than alpha-beta alloys.

Another desirable effect of the slow rate of transformation in beta alloys is that it can attain uniform properties in thick sections. Alpha-beta alloys like Ti-6Aℓ-4V are quite quench sensitive, and uniform high strength conditions can be achieved only in thin sections by rapid quenching. In deep hardening alloys, because of the slow cooling rate that can be used without affecting the mechanical properties, the residual stresses arising out of fast quenching also are avoided.

The beta alloys have great potential for developing high strength and fracture toughness by developing suitable microstructures. Due to the higher content of beta stabilizers, the amount of α precipitated in beta alloys is less than that in alpha-beta alloys, and the rate of transformation is slow. Hence, in principle, a wide

range of strength and toughness can be obtained in these alloys by controlled decomposition of ß. The structure of the precipitates and their distribution depend on the composition of the alloy and the ageing temperature [2,3]. During ageing at high temperature α is precipitated directly from ß by heterogeneous nucleation along grain boundaries and dislocations. At low temperatures intermediate precipitate ω or ß' is formed depending on composition. In beta alloys containing relatively low amount of beta stabilizers the intermediate precipitate is the ω phase; whereas in those with high alloy content the intermediate phase is ß'. The precipitation of ω as well as ß' is homogeneous. Since the cost of beta alloys increases with the amount of ß stabililzing elements, the beta alloys developed are those that have ω as the low temperature precipitate. The ω precipitates are fine and the precipitation is intense. Hence, the alloy hardens rapidly and becomes brittle. Control of precipitation in the early stages to achieve an acceptable toughness is difficult. It has been suggested that the ω phase be completely avoided and α be precipitated directly at high temperatures [4]. The problem of heterogeneous precipitation of α can be partially solved by deforming the material and precipitation hardening without allowing the material to recrystallize. This will provide a dense network of dislocations as nucleation sites for α.

Another probable approach is to harden the alloy initially by ω precipitation, and then age the brittle alloy at high temperature to increase toughness. During this process, ω precipitates dissolve and "in situ" precipitation of α takes place homogeneously. Thus, a combination of high strength and high toughness may be obtained due to homogeneous distribution of precipitates. A combination of working and duplex ageing may yield a higher toughness. A detailed study of these thermomechanical treatments have not been performed on the ß alloys.

The recently developed ß titanium alloy, Ti-15-3 (Ti-15V-3Cr-3Aℓ-3Sn) seems to have the potential to become an important aircraft structural alloy both in sheet form and thick sections. The density of Ti-15-3 is 4.76gm/cc compared to 4.54gm/cc for titanium. Its forming characteristics equal that of commercial purity titanium, and it can be produced in strips with improved uniformity with respect to dimensional tolerance, surface finish and mechanical properties [1]. The microstructural changes in Ti-15-3 and their effect on strength and fracture toughness have not been examined in detail.

The purpose of this investigation was to examine the mechanical property changes in the Ti-15-3 alloy resulting from heat treatments at various temperatures, and to study the underlying microstructures in selected cases, so that

methods of developing suitable microstructures for structural applications can be established. Single-stage heat treatments at various temperatures including low temperature ageing, where the ω phase is precipitated, and high temperature ageing, where the α phase is precipitated, were studied along with various duplex ageing treatments.

EXPERIMENTAL PROCEDURE

The Ti-15-3 alloy was obtained from TIMET Corporation in the form of 1.5in. thick plates in hot rolled condition. It was processed by TIMET by press forging at 2000°F from 8in. diameter to 5" x 6" x L, at 1700°F to 2" x 6" x L and hot rolled from 1700°F without heating to 1-1/2" in 5 passes. The alloy had the chemical composition: V - 14.79%, Aℓ-2.91%, Cr-3.06%, Sn-3.03%, Fe-0.128%, O_2-0.122%, N_2-0.009% and balance titanium. The β transus temperature for this alloy is between 1385°F and 1415°F.

A wide variety of heat treatments were used. Single-stage ageing was performed in the temperature range 500-1050°F. The multiple ageing treatments involved combinations of low temperature ageing between 600°F and 800°F and high temperature ageing between 1000°F and 1125°F. In a few cases the ageing treatment was preceded by a solution treatment at 1500°F. After each step of the ageing or solution treatment the specimen was cooled in air. The heat treatment was performed in a box furnace in atmospheric air. Due to the likely contamination of surface by oxygen during heat treatment, specimens were prepared after removing a thick layer of the material by machining.

Although the correlation between hardness values and tensile properties of titanium alloys is not as good as in steel, hardness measurement was used for monitoring progress of ageing because of the ease of measurement. Rockwell scale D was used for hardness determination. From the hardness curves so obtained, heat treatments were chosen for tensile property determination. Tensile tests were performed on 0.25in. diameter, ASTM standard sub size specimens, the test machine being operated in displacement control. The heat treatments that produced promising combinations of strength and ductility were selected for fracture toughness determination. One-inch thick compact tension specimens (1T, W = 2in.) were tested according to ASTM Standard E399.

The microstructural changes causing the changes in mechanical properties were studied using optical, scanning and transmission electron microscopy. Variations in grain size and size, shape and distribution of second phase particles were examined.

RESULTS AND DISCUSSION

The ageing treatments were chosen to assess the hardening characteristics due to precipitation of the ω phase at low temperatures, the α phase at high temperatures, and due to duplex ageing. The hardening curves for single-stage ageing at different temperatures are given in Fig. 1 and 2. The curves show that the nose of the Time-Temperature Transformation (TTT) curve for the ω phase is in between 600°F and 700°F as the ageing time needed to reach peak hardness is the least at these temperatures. The peak hardness remains essentially the same between 500°F and 700°F and drops with further increase in ageing temperature. This drop is not attributed to the change in the size of the ω particles, but due to the transition from ω particles to α particles. The shape of the TTT curve for α cannot be inferred from the hardness measurements alone as the hardness decreases due to the increase in the precipitate size. A detailed microstructural analysis was not attempted to study the rate of α precipitation. The ageing treatment at 1050°F was preceded by a solution treatment at 1500°F, but the solution treatment does not seem to have changed the general trend in ageing behavior.

The results of various duplex ageing treatments are shown in Fig. 3 and 4. There was no increase in hardness

in 6 hours at 600°F, but it is not clear whether the nucleation at this stage had influenced subsequent ageing at higher temperatures. Ageing at 600°F for 48 hours resulted in peak hardness (Fig. 1), and further ageing at 1050°F resulted in softening (Fig. 3). The solution treatment at 1500°F before ageing treatment did not change the hardening characteristics during duplex ageing also (Fig. 3). High temperature ageing (1000°F and 1100°F) after ageing for 24 hours at 700°F (Fig. 4) shows an initial drop in the hardness, the extent of the drop being dependent on the final ageing temperature, after which the hardness remains essentially steady for a long period of time. However, after ageing for 48 hours at 600°F (Fig. 3) or 24 hours at 800°F (Fig. 4), decrease in hardness during high temperature ageing in gradual, indicating that the structures formed at low temperature ageing are more stable than that formed during 24 hours ageing at 700°F. Ageing at 800°F produces a stable structure more rapidly than at 600°F and 700°F.

Heat treatments for tensile tests were chosen based on the hardness values, encompassing a wide range of strength levels. More emphasis was given to the intermediate strength levels. To obtain repeatable results, ageing time periods, during which the strength changed rapidly, were avoided. The tensile test results are presented in Table 1. As indicated by the hardness values, the higher

ageing temperatures produced lower strength and correspondingly higher elongation at fracture. However, heat treatments that yielded the same hardness values were found to yield slightly different strength values.

A comparison of the tensile properties after single-stage ageing and duplex ageing can be made by studying the ductility as a function of yield strength or tensile strength. However, the comparison is limited in scope as the single-stage ageing treatments chosen produced strength values at the higher and lower ends of the range of strength values, whereas duplex ageing produced intermediate strength values. Furthermore, duplex ageing showed more scatter in ductility. Plots of yield strength and tensile strength versus ductility are shown in Fig. 5 and Fig. 6 respectively. In duplex ageing, where the low temperature ageing produced a relatively stable structure (800°F/24 hrs, 600°F/48 hrs), subsequent high temperature ageing resulted in relatively good ductility, but appeared to be slightly inferior to single-stage ageing. Duplex ageing in which the low temperature ageing produced relatively unstable structure (600°F/6 hrs, 600°F/24 hrs, 700°F/24 hrs) rendered the material inferior in ductility.

Some additional multiageing sequences were examined. In one, ageing for 24 hours at 1000°F was followed by 24 hours at 800°F resulted in good ductility at intermediate strength level (Table 1). A triple ageing treatment,

800°F/6 hours + 1075°F/8 hours + 1125°F/18 hours, also resulted in desirable combination of strength and ductility.

The fracture toughness values were determined only for a few promising microstructures. Only one test was performed for each structure. However, the test results showed that multiageing treatments (HT 17,19,20,21) yielded fracture toughness values superior to those of single stage ageing when compared on the basis of yield strength. This is evident from Table 2 and the plot of fracture toughness versus yield strength in Fig. 7a. Only heat treatment 20 did not meet the ASTM Standard E399, since P_{max}/P_q exceeded 1.1 (P_{max}/P_q = 1.15). It indicates that K_{Ic} for heat treatment 20 is slightly higher than 65.05 MPa$\sqrt{m}$. The data for multiaged alloy and single stage aged alloy follow the general trend exhibited by other titanium alloys. The data along with those reported for other titanium alloys [6,7] are plotted in Fig. 7b. The Ti-15-3 results are within the technological limits of other titanium alloys, the multiageing treatment yielding values near the top of the toughness range. The results of Ti-15-3 were also compared with those from Ti-10-2-3 alloy [8], which has become prominent recently. Figure 7c shows that Ti-15-3 compares favorably with Ti-10-2-3.

The microstructures of Ti-15-3 after different heat treatments were studied to investigate their influence on

the mechanical properties. The grain size of the alloy remained essentially the same for all the structures. A typical grain structure is shown in Fig. 8. Optical microstructures of heat treatments (HT), 1,2,3,4,17,19 and 20 are shown in Fig. 9. The microstructures of 1,17 and 19 are not resolved at this magnification, indicating fine precipitation resulting in high strength. In HT2 the grain boundary α precipitates are needle shaped, but the structure in the interior of the grain is not resolved. This structure formed at 900°F showed relatively high strength. In ageing 1000°F (HT3) the coarser structure formed is resolved under the microscope, and the strength is lower. The 1050°F structure (HT4) is even coarser. The high temperature ageing followed by low temperature ageing (HT20) produced a mixture of coarse and fine needles, which yielded a good combination of strength and ductility. A few of the microstructures were also examined under a scanning electron microscope at higher magnifications. However, these studies did not reveal more useful information, and hence, scanning microscopic study was not pursued further.

A limited transmission electron microscopic study of four selected microstructures was performed. These were the as received alloy, the alloy aged for 24 hours at 700°F, that aged for 48 hours at 1000°F, and that was duplex aged for 24 hours at 700°F + 24 hours at 1050°F. The alloy in the as received condition had low dislocation density

(Fig. 10) indicating a fully recrystallized condition after hot working. No precipitate particles were visible, but streaks were observed in diffraction patterns apparently due to beginning of nucleation of second phase particles. After 24 hours of ageing at 700°F the precipitates were still not resolved, but had a mottled appearance, Fig. 11. This was probably due to the very small size of the precipitates or due to the large thickness of the foil used. The diffraction pattern revealed two structures, indicating the formation of precipitates. After ageing for 48 hours at 1000°F the precipitates were large and elongated, Fig. 12. These are considered to be α particles. In the duplex aged condition the precipitates had a bimodal distribution, Fig. 13. Although the sizes of the precipitates were different, the shapes were similar.

The beginning of nucleation as indicated by streaks in the diffraction patterns of the alloy in the as received condition was probably caused by slow cooling after hot working. Slow cooling also may have drained excess vacancies. This may account for the higher strength obtained when ageing is performed after solution treatment. Although the specimens are air-cooled after solution treatment, cooling is faster as the specimen size is much smaller than that of the plate. After ageing for 24 hours at 700°F the precipitates are very small. The immediate softening on subsequent ageing can be attributed

to rapid dissolution of the tiny precipitates. Apparently larger and more stable precipitates are formed on prolonged low temperature ageing. The bimodal distribution of the precipitates on high temperature ageing after short time low temperature ageing does not explain the low ductility in this condition. Similarly, the improvement of ductility due to extended low temperature ageing before high temperature ageing is not understood. The higher fracture toughness of the duplex aged alloys compared to single-stage aged ones is more intriguing. Additional microstructural study will be needed to understand the factors involved in these property changes.

CONCLUSIONS

From the study of various heat treatments and their effects on microstructure and mechanical properties of the beta titanium alloy, Ti-15-3, the following conclusions have been reached:

1. Ti-15-3 can be heat treated to obtain a wide range of strength levels, with corresponding variation in ductility from high ductility at low strength to almost brittle behavior at high strength.
2. Attractive combinations of strength and fracture toughness can be attained at medium and high strength levels by suitable heat treatment. The toughness data obtained from multiageing treatments fall at the upper end of the fracture analysis diagram for titanium alloys.
3. Multiageing treatments consistently produced higher fracture toughness than single-stage ageing at any given strength level. However, smooth specimen tensile ductility did not exhibit this trend.
4. The typical microstructure - mechanical property relationships observed in other alloy systems, increase in strength and decrease in ductility with decreasing precipitate size, is observed in this titanium alloy as well.

5. The low temperature decomposition product (ω) is very unstable on subsequent ageing at high temperature, unless the low temperature ageing has proceeded for a long period. When the low temperature phase is more stable, duplex ageing yields higher ductility than when the low temperature phase is unstable. The microstructural changes causing this difference were not investigated due to the limited scope of the study. Additional microstructural studies should help to develop additional heat treatments yielding even more desirable mechanical properties.

REFERENCES

[1] Preliminary Properties of Ti-15-3 TIMET, November, 1977.

[2] J. C. Williams: Titanium Science and Technology, JAFFEE and Burte, eds., Plenum Press, New York, 1973, p. 1433.

[3] J. C. Williams, F. H. Froes and C. F. Yolton, Met. Transactions, Vol. 11A, p. 356, 1978.

[4] F. H. Froes et al., Met. Transactions, Vol. 11A, p. 21, 1980.

[5] G. R. Keller, J. C. Chesnutt, F. H. Froes and C. A. Rhodes, Naval Air Systems Command Report NA-78-917, December 1978.

[6] W. S. Pellini, "Principles of Structural Integrity Technology," Office of Naval Research, 1976.

[7] R. W. Judy, Jr. and R. J. Goode, Screening Test Method Development for Fracture Resistance Measurements in Thin Gage Titanium, "Toughness and Fracture Behavior of Titanium," ASTM, STP 651, pp. 217-226.

[8] The Aerospace Structural Metals Handbook, Vol. 4, p. 43.

TABLE 1

Tensile Properties of Different Microstructures

Heat Treatment*	Elastic Modulus GPa (10^6 psi)	Yield Strength MPa (ksi)	UTS MPa (ksi)	% Elongation
1	101.8 (14.76)	1423 (206.4)	1469 (213.1)	2.00
2	104.7 (15.18)	1273 (184.6)	1340 (194.4)	4.38
3	98.7 (14.31)	1043 (151.3)	1128 (163.6)	9.97
4	105.8 (15.34)	966 (140.1)	1061 (153.9)	12.72
5	103.0 (14.94)	957 (138.8)	1031 (149.5)	5.19
6	99.3 (14.40)	999 (144.9)	1082 (156.9)	7.34
7	97.7 (14.17)	1024 (148.5)	1097 (159.1)	5.64
8	108.8 (15.78)	1054 (152.9)	1123 (162.9)	4.60
9	98.2 (14.24)	1060 (153.7)	1118 (162.2)	5.16
10	103.0 (14.94)	1085 (157.3)	1152 (167.1)	7.05
11	98.7 (14.32)	1093 (158.5)	1158 (167.9)	5.94
12	97.8 (14.19)	1103 (159.9)	1167 (169.2)	4.23
13	101.8 (14.76)	1171 (169.9)	1228 (178.1)	3.54
14	98.5 (14.18)	1132 (164.2)	1191 (172.7)	3.80
15	99.3 (14.40)	1296 (188.0)	1324 (192.0)	2.23
16	105.8 (15.35)	1265 (183.4)	1314 (190.6)	2.94
17	101.0 (14.65)	1193 (173.0)	1249 (181.2)	4.64
18	93.4 (13.55)	1143 (165.7)	1204 (174.6)	4.25
19	95.6 (13.87)	1076 (156.0)	1142 (165.6)	6.36
20	105.4 (15.28)	1120 (162.4)	1218 (176.6)	7.00
21	97.6 (14.15)	1055 (153.0)	1139 (165.2)	7.13

* Details of heat treatments are on the following page.

Table 1

(Continued)

*Heat Treatment

1. 800°F (427C)/24hrs
2. 900°F (482C)/24hrs
3. 1000°F (538C)/48hrs
4. 1050°F (566C)/24hrs
5. 1500°F (816)/1/2hr + 1050°F (566C)/16hrs
6. 1500°F (816C)/1/2hr + 1050°F (566C)/24hrs
7. 600°F (316C)/6hrs + 1050°F (566C)/16hrs
8. 600°F (316C)/6hrs + 1050°F (566C)/48hrs
9. 600°F (316C)/24hrs + 1050°F(566C)/24hrs
10. 600°F (316C)/48hrs + 1050°F (566C)/24hrs
11. 600°F (316C)/48hrs + 1050°F (566C)/32hrs
12. 1500°F (816C)/1/2hr + 600°F (316C)/24hrs + 1050°F (566C)/24hrs
13. 1500°F (816C)/1/2hr + 600°F (316C)/48hrs + 1050°F (566C)/12hrs
14. 1500°F. (816C)/1/2hr + 600°F (316C)/48hrs + 1050°F (566C)/16hrs
15. 700°F (371C)/24hrs + 1000°F (538C)/6hrs
16. 700°F (371C)/24hrs + 1000°F (538C)/24hrs
17. 850°F (427C)/24hrs + 1050°F (566C)/6hrs
18. 800°F (427C)/24hrs + 1050°F (566C)/24hrs
19. 800°F (427C)/24hrs + 1100°F (593C)/4hrs
20. 1000°F (538C)/24hrs + 800°F (427C)/24hrs
21. 800°F (427C)/6hrs + 1075°F (579C)/8hrs + 1125°F (607C)/18hrs

TABLE 2

Fracture Toughness and Tensile Properties

Of Selected Microstructures

Heat Treatment	Yield Strength MPa (ksi)	UTS MPa (ksi)	% Elongation	Fracture Toughness MPa$\sqrt{m}$ (ksi$\sqrt{in.}$)
2	1273 (184.6)	1340 (194.4)	4.38	47.45 (43.18)
3	1043 (151.3)	1128 (163.6)	9.97	48.88 (44.48)
4	966 (140.1)	1061 (153.9)	12.72	61.20 (55.69)
17	1193 (173.0)	1249 (181.2)	4.64	61.14 (55.64)
19	1076 (156.0)	1142 (165.6)	6.36	69.89 (63.60)
20	1120 (162.4)	1218 (176.6)	7.00	65.05 (59.20)*
21	1055 (153.0)	1139 (165.2)	7.13	76.70 (69.80)

* Did not meet ASTM E399 requirement, as $\frac{P_m}{P_q} = 1.15$.

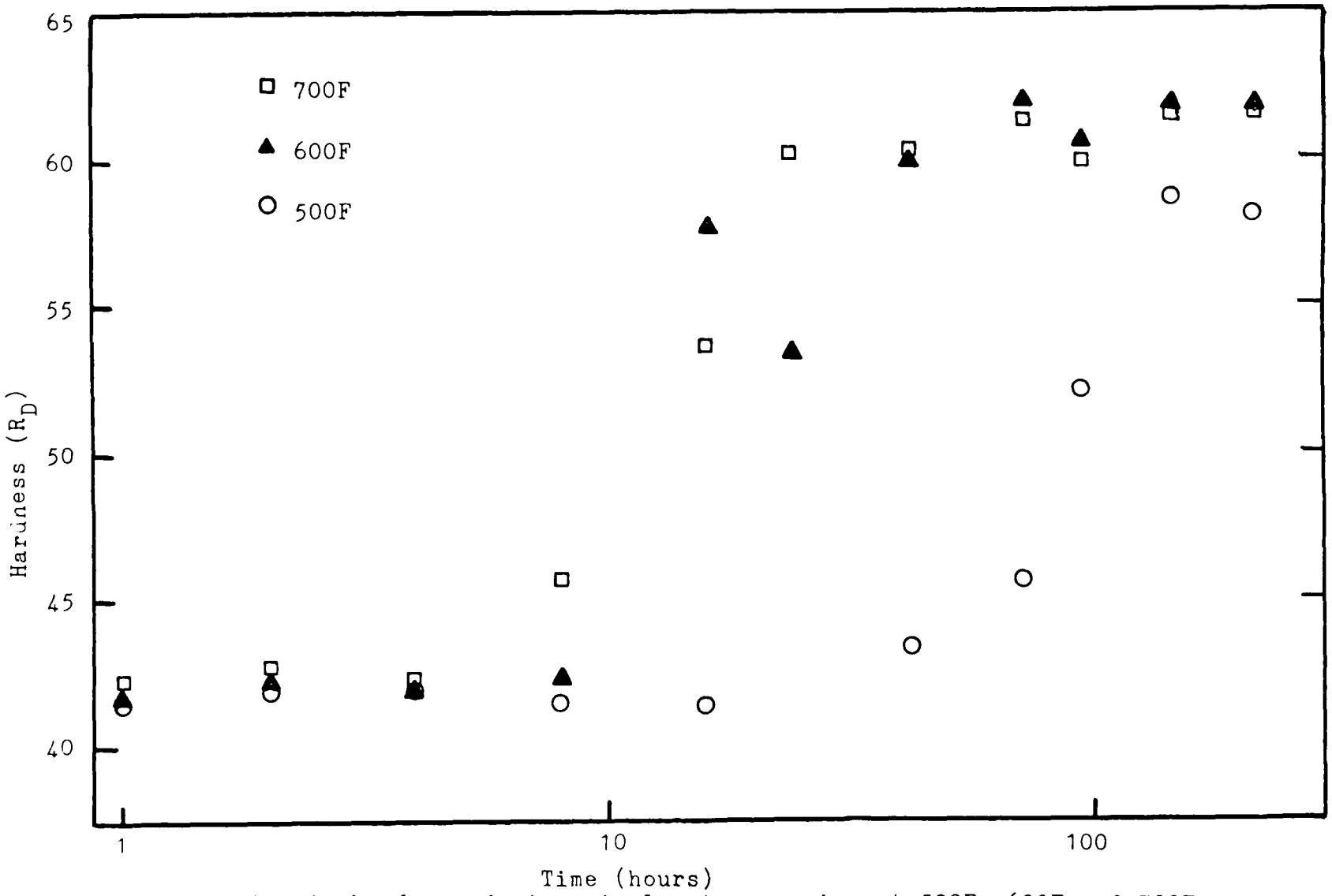

Fig. 1. Variation in hardness during single stage ageing at 500F, 600F and 700F.

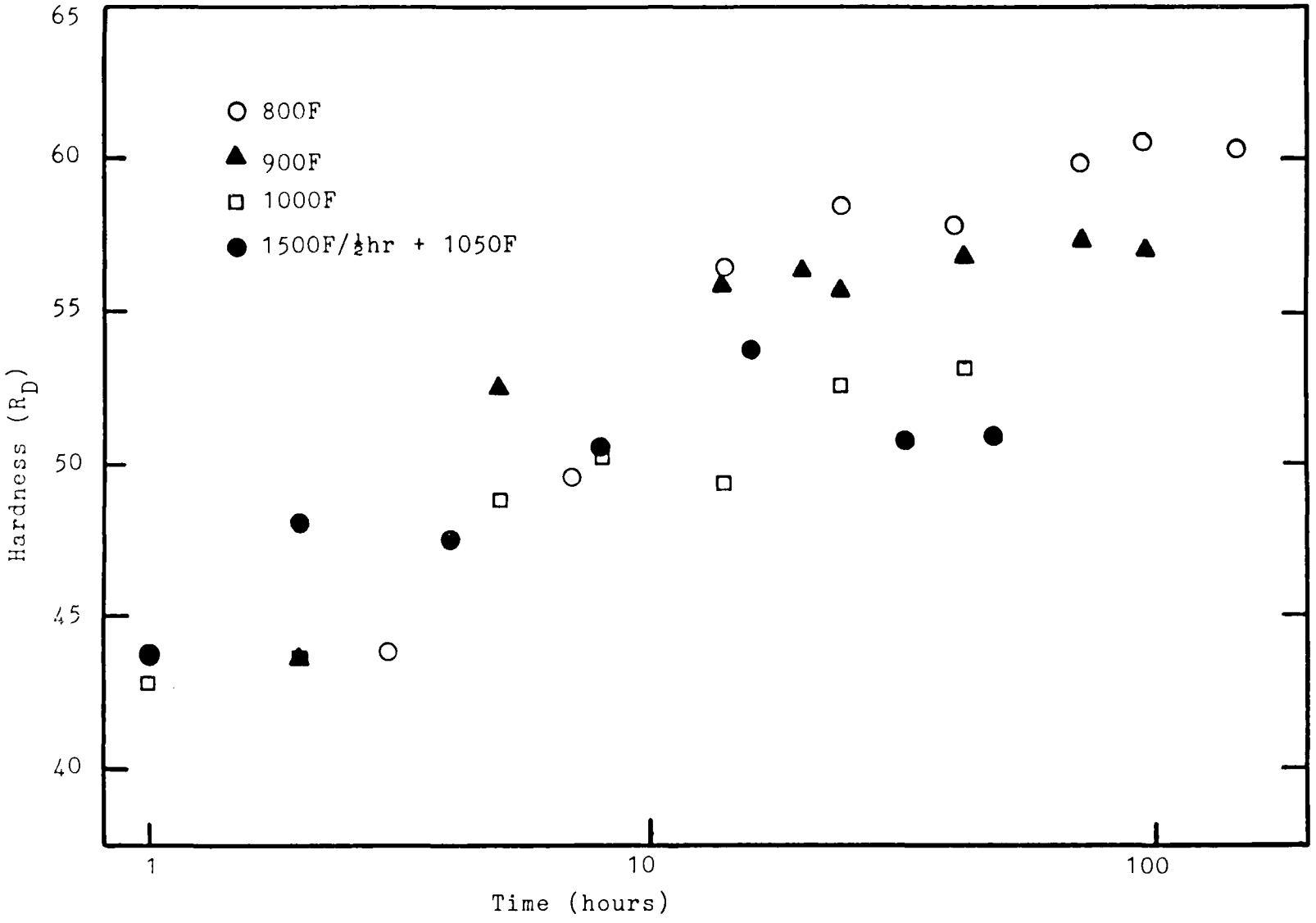

Fig. 2. Variation in hardness during single stage ageing at 800F, 900F, 1000F and 1050F.

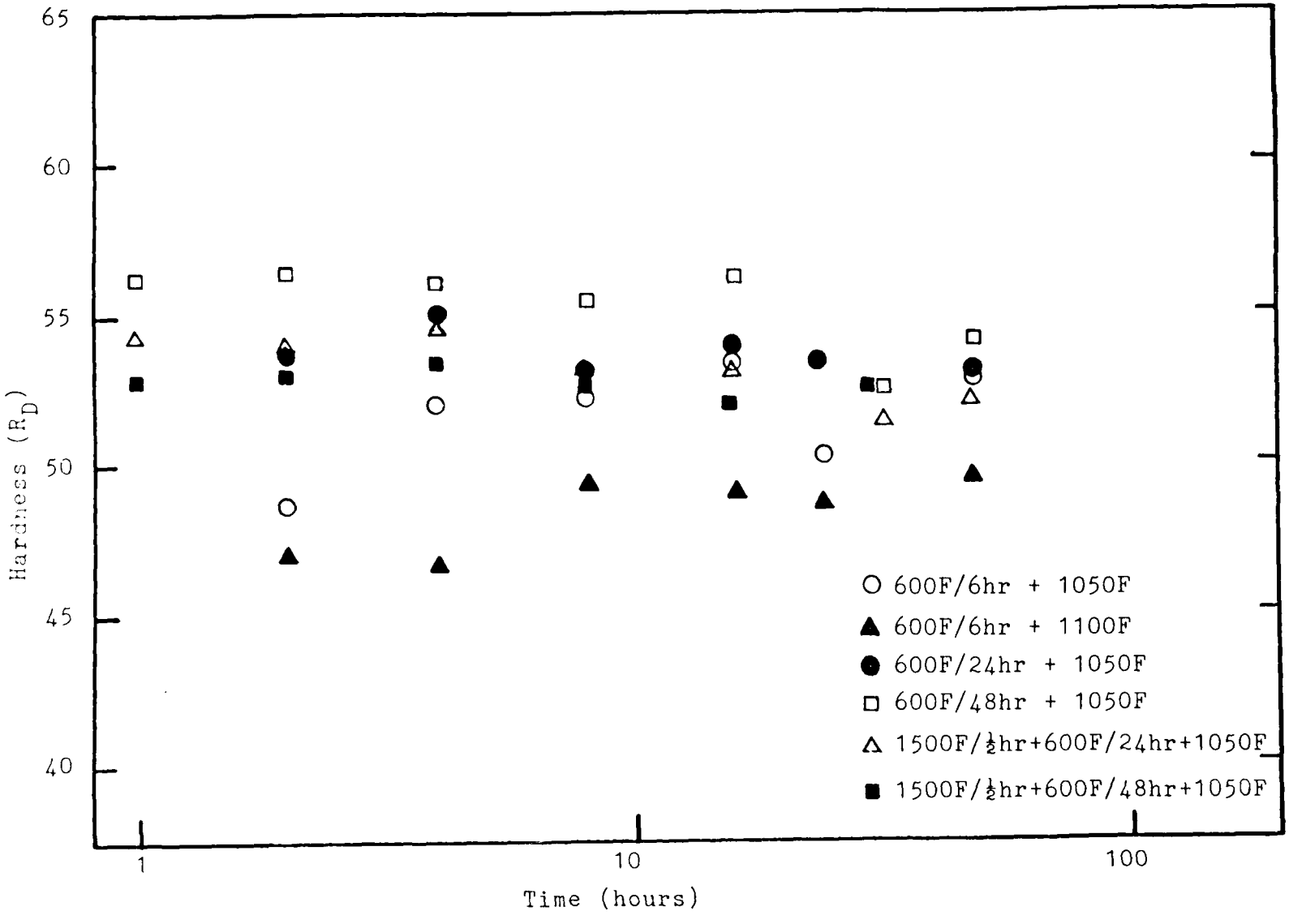

Fig. 3. Variation in hardness during duplex ageing after preageing at 600F.

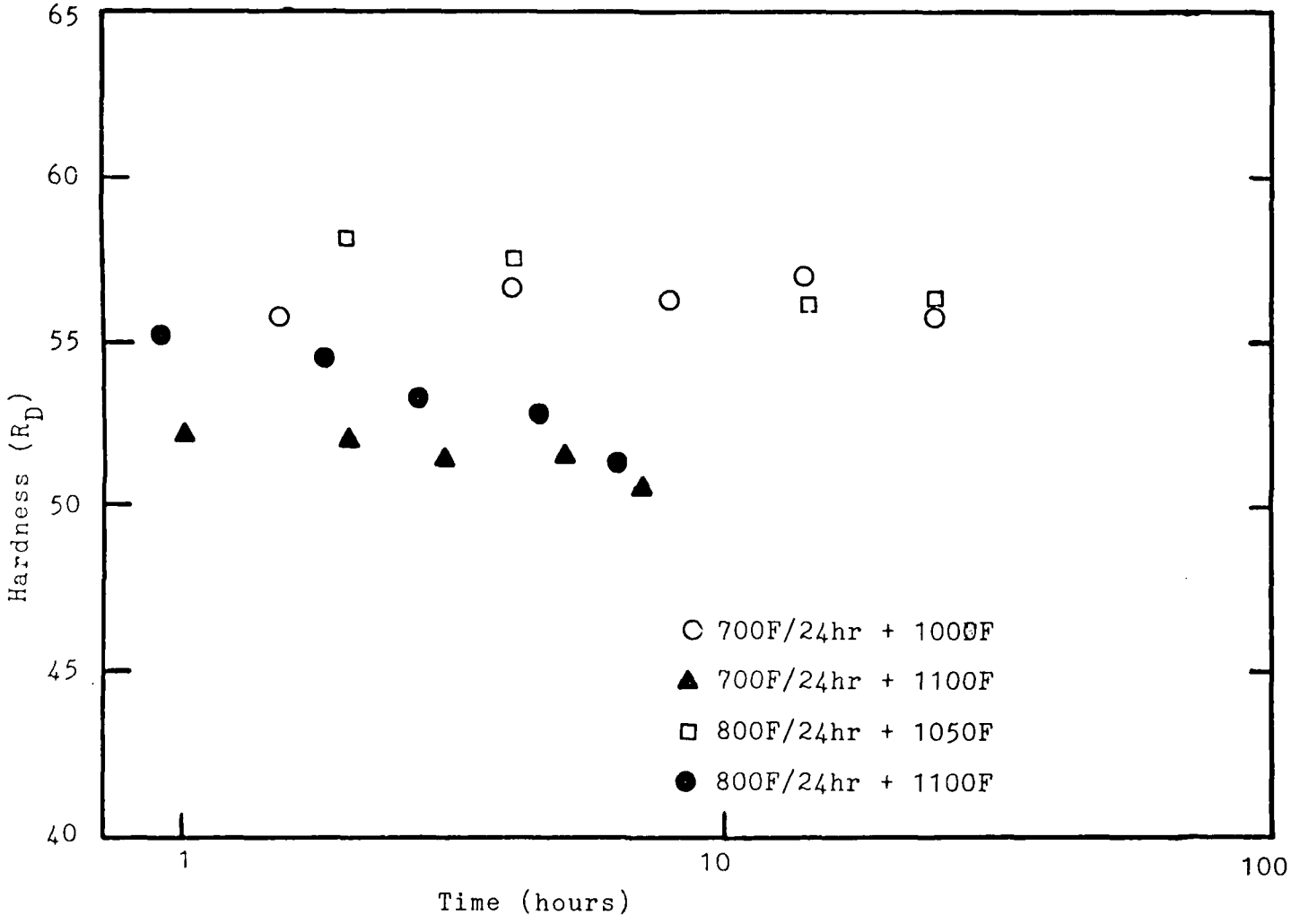

Fig. 4. Variation in hardness during duplex ageing after preageing at 700F and 800F.

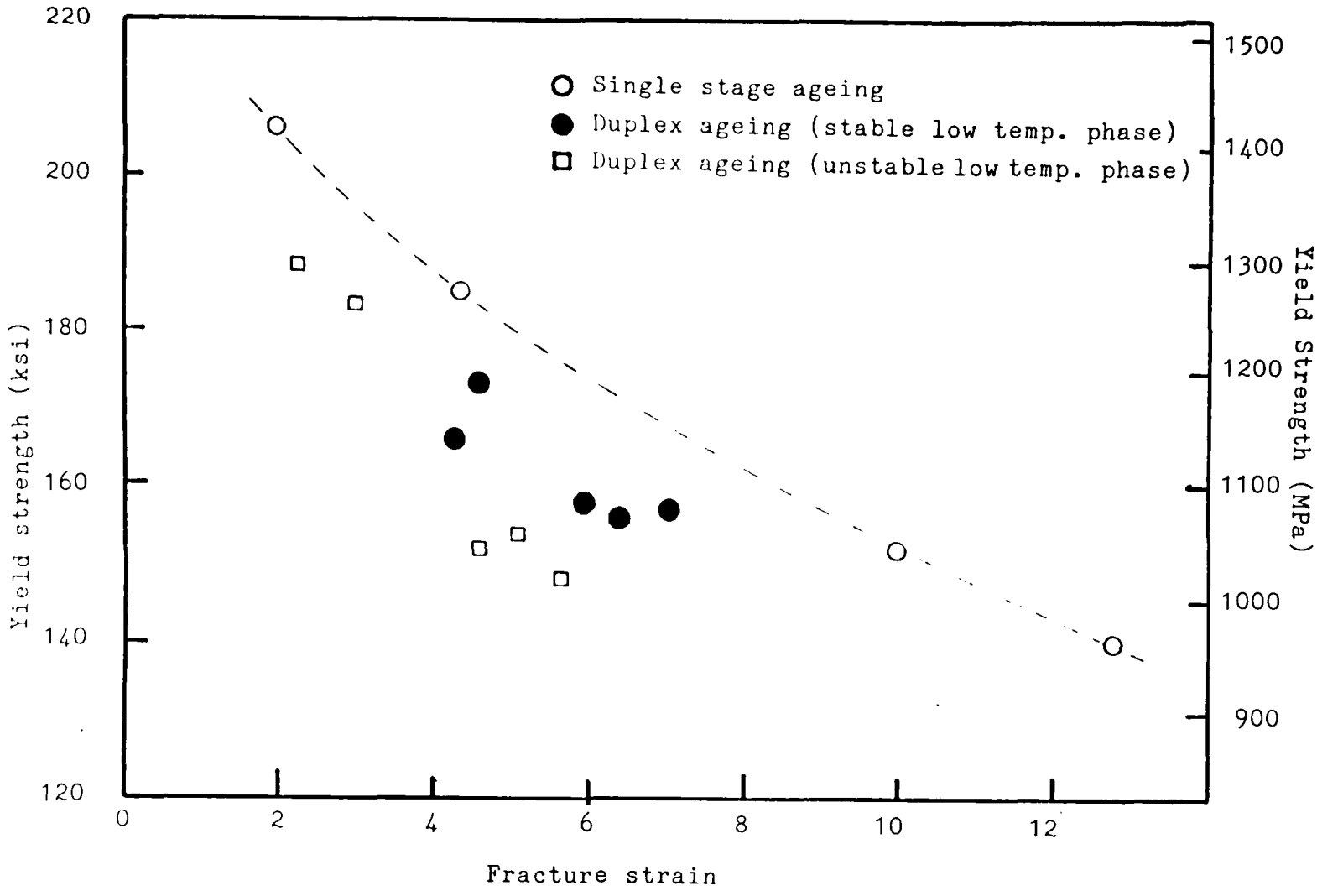

Fig. 5. Variation in yield strength and ductility with different heat treatments.

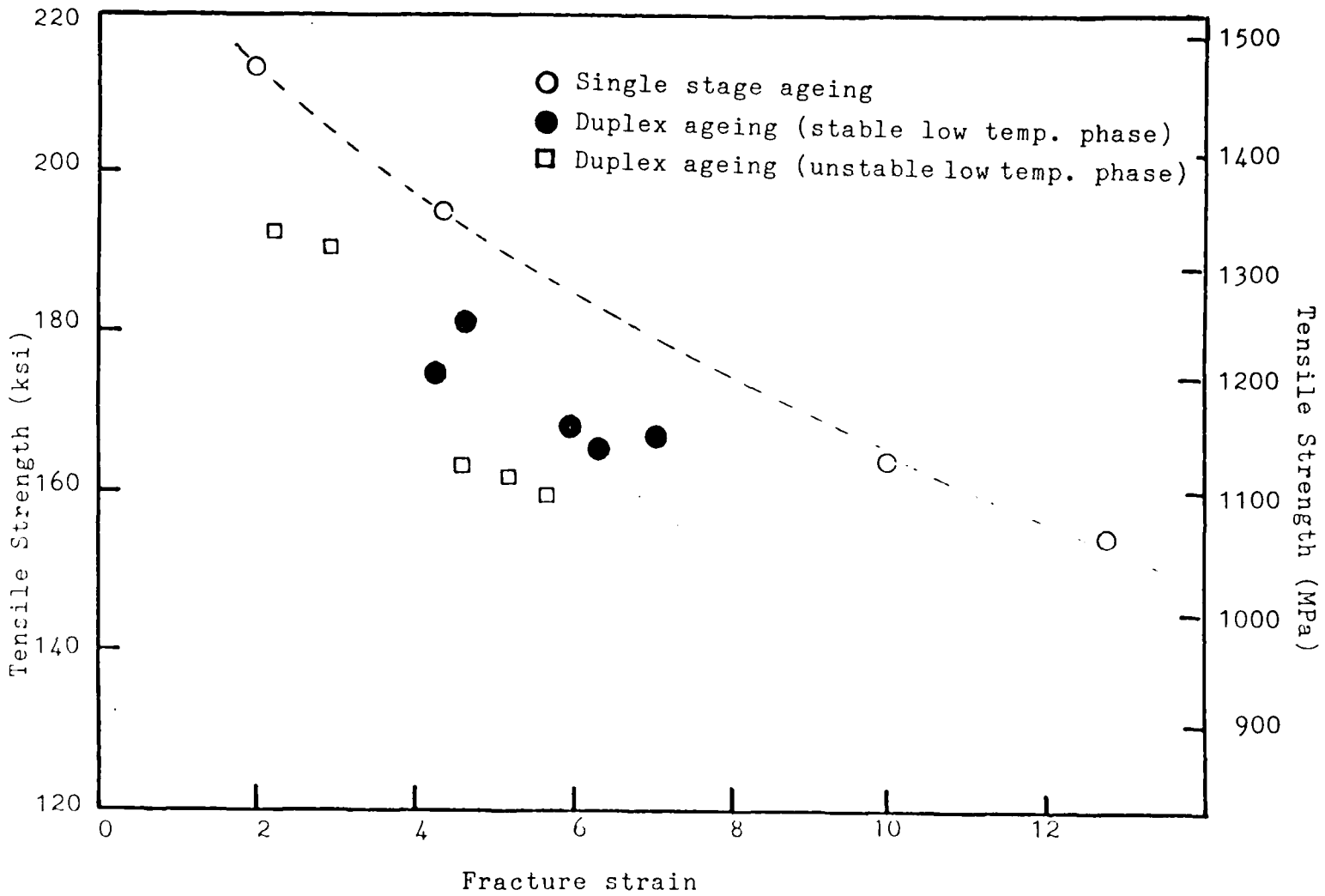

Fig. 6. Variation in ultimate tensile strength and ductility with different heat treatments.

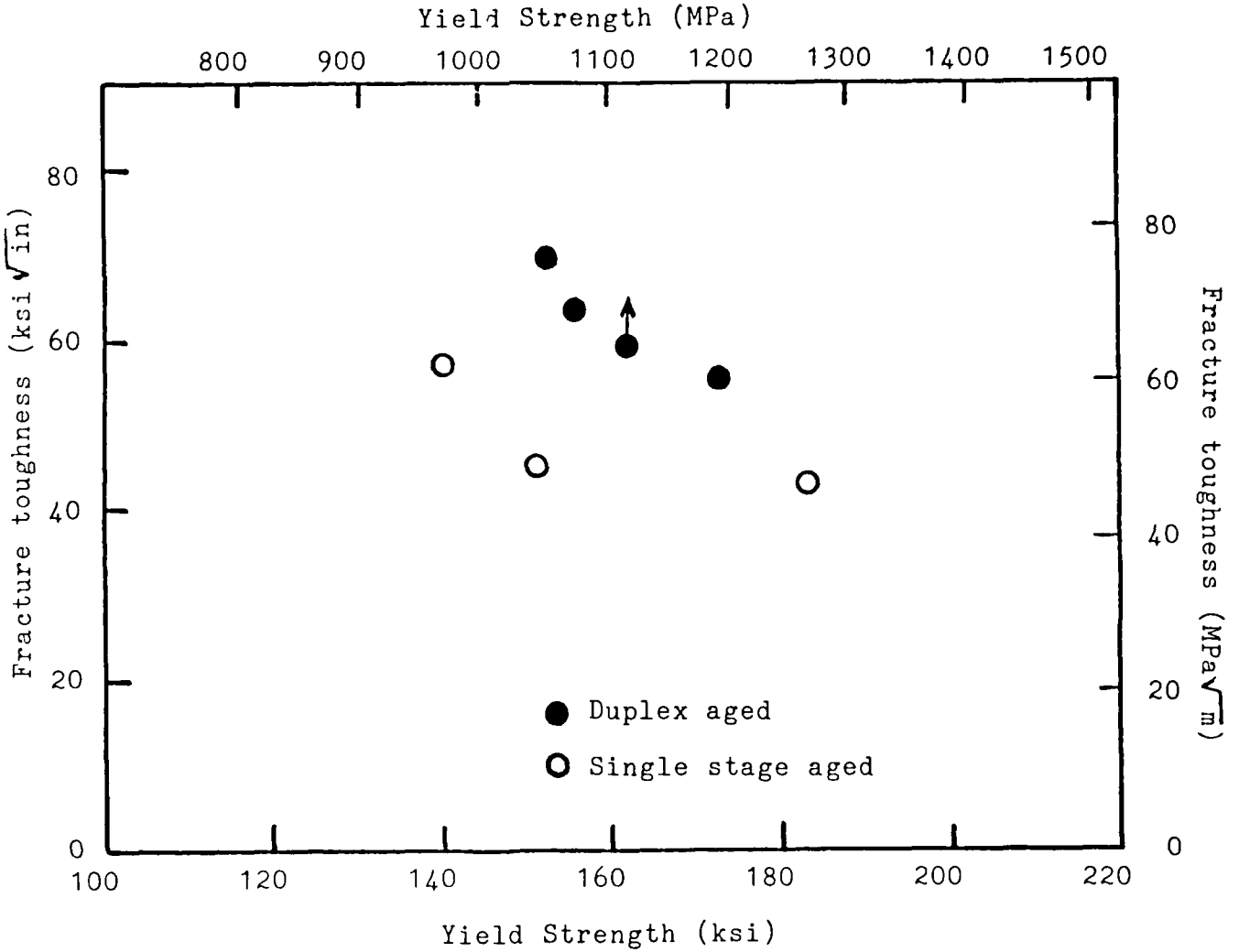

Fig. 7A. Effect of ageing treatment on yield strength and fracture toughness.

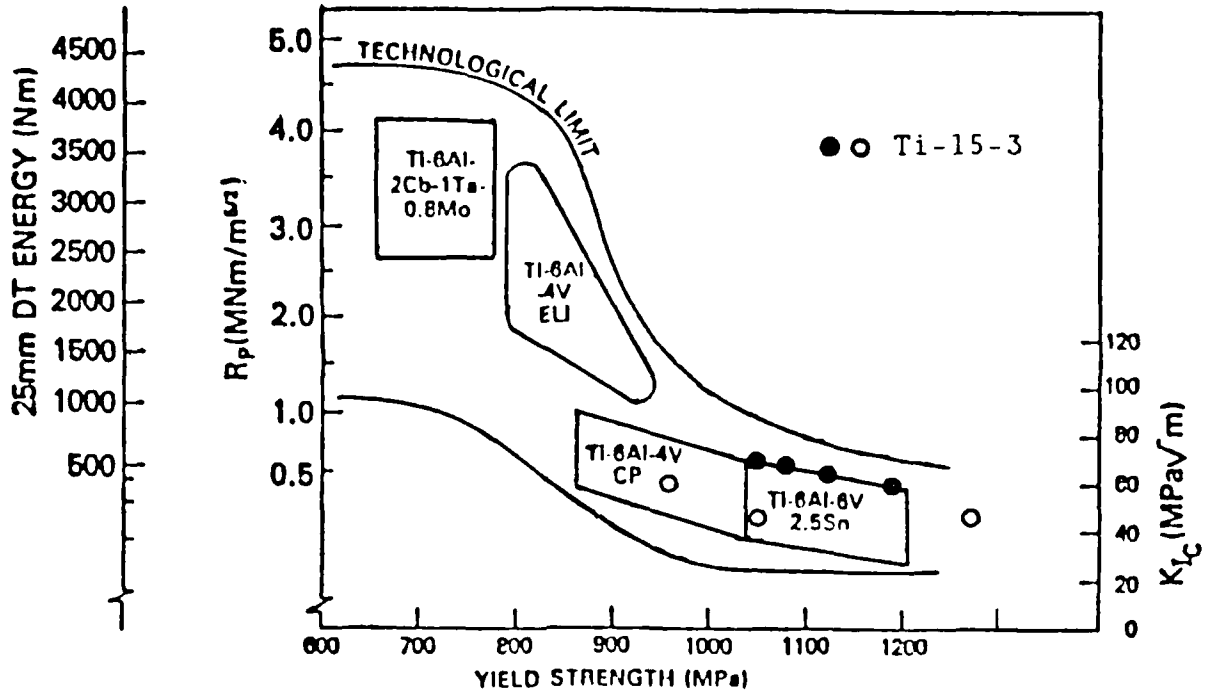

Fig. 7B. Ratio analysis diagram for titanium alloys with new data from Ti-15-3 alloy.

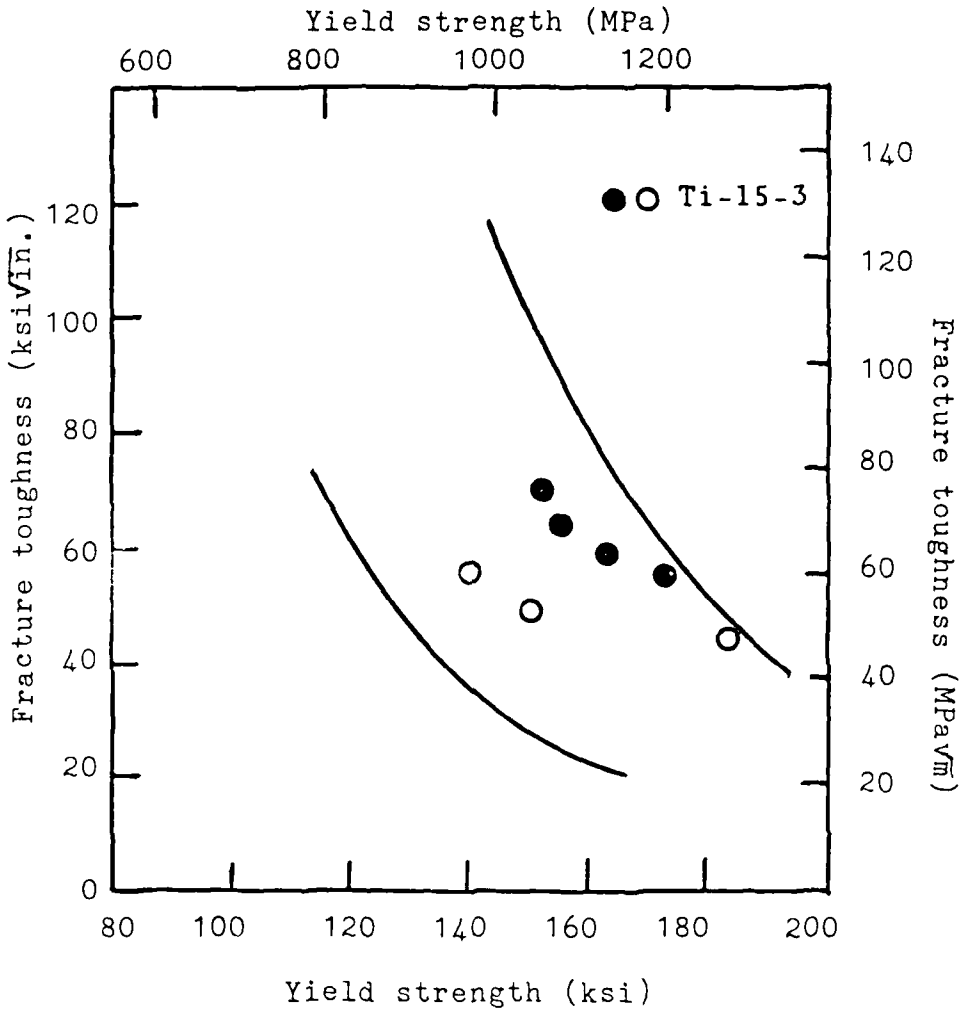

Fig. 7C. Comparison of fracture toughness of Ti-10-2-3 alloy with new data from Ti-15-3 alloy.

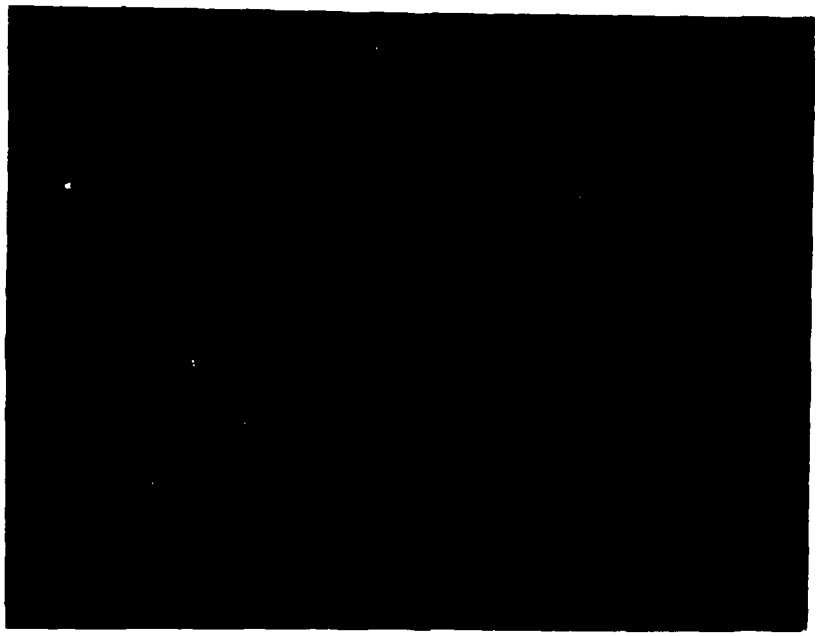

Fig. 8. A typical grain size distribution after ageing treatment (100x)

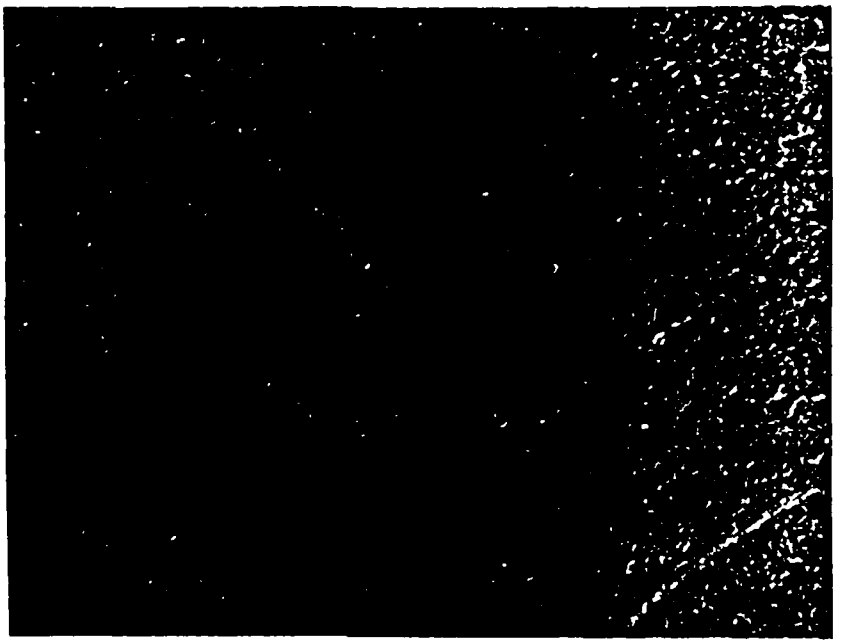

Fig. 9 - HT1

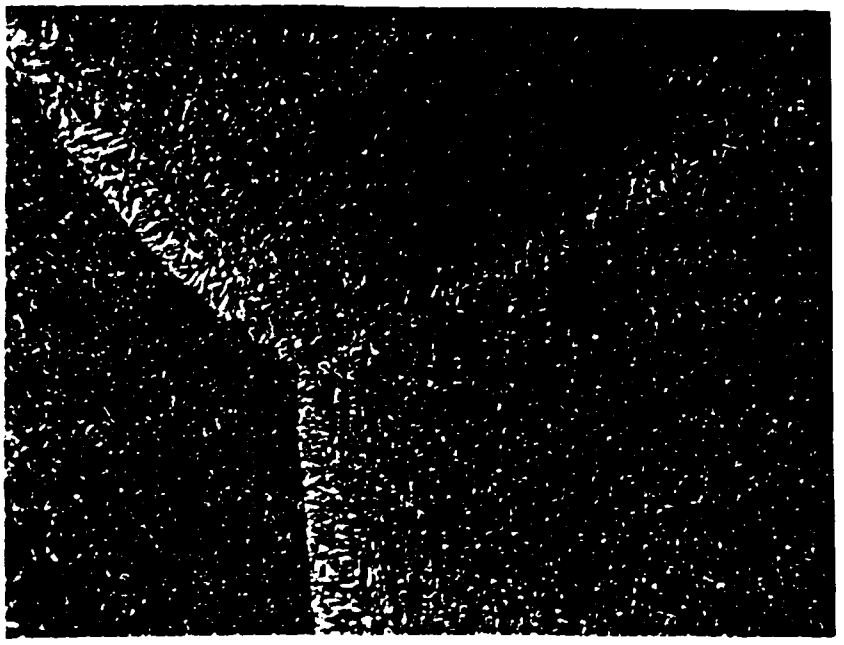

Fig. 9 - Ht2

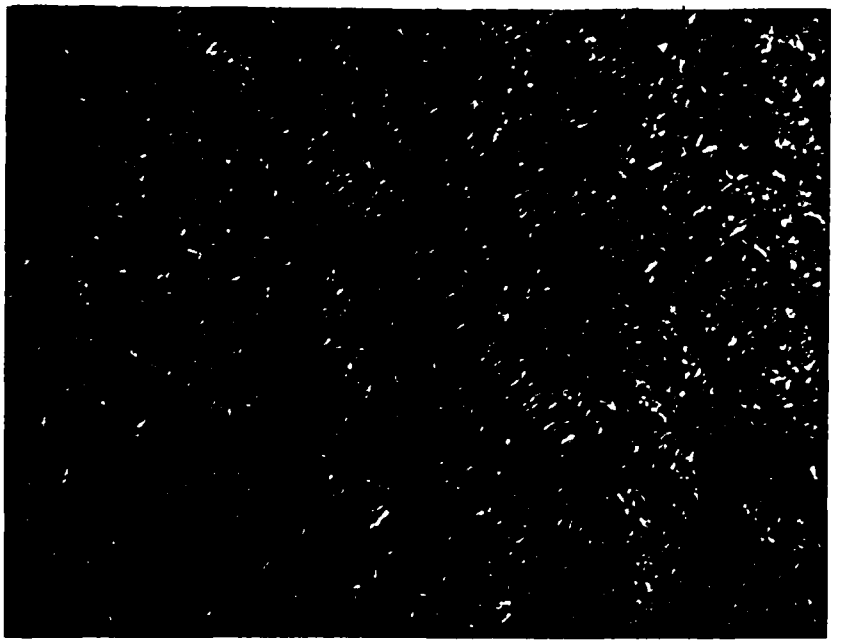

Fig. 9 - HT3

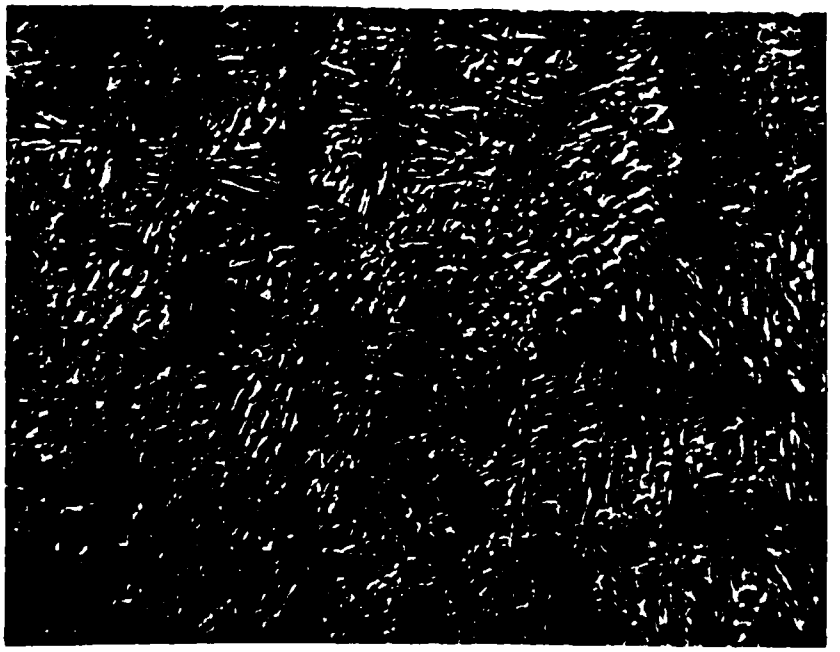

Fig. 9 -HT4

Fig. 9 - HT17

Fig. 9 - HT19

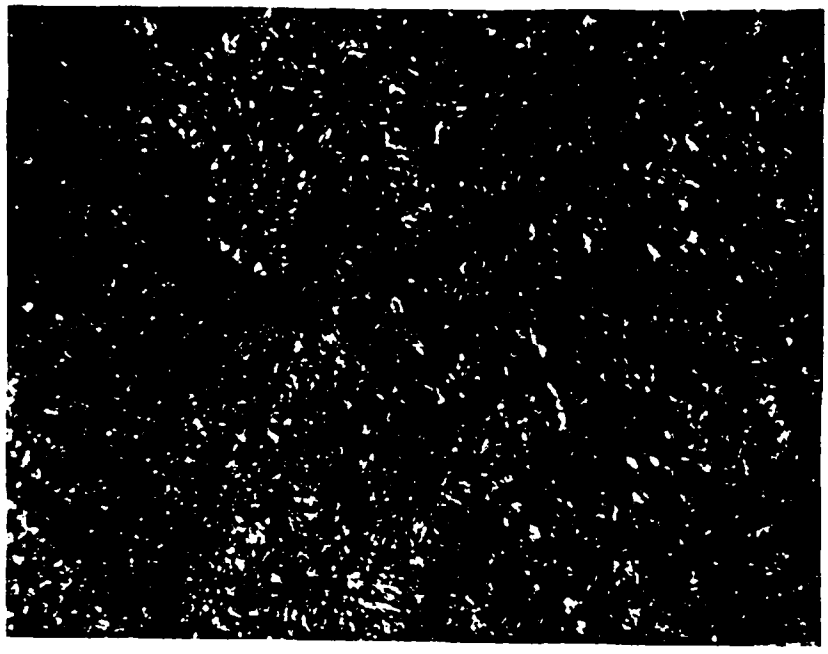

Fig. 9 - HT20

Fig. 9. Microstructures after different heat treatments (1000x)

Fig. 10. Transmission electron micrograph, as received (31500X)

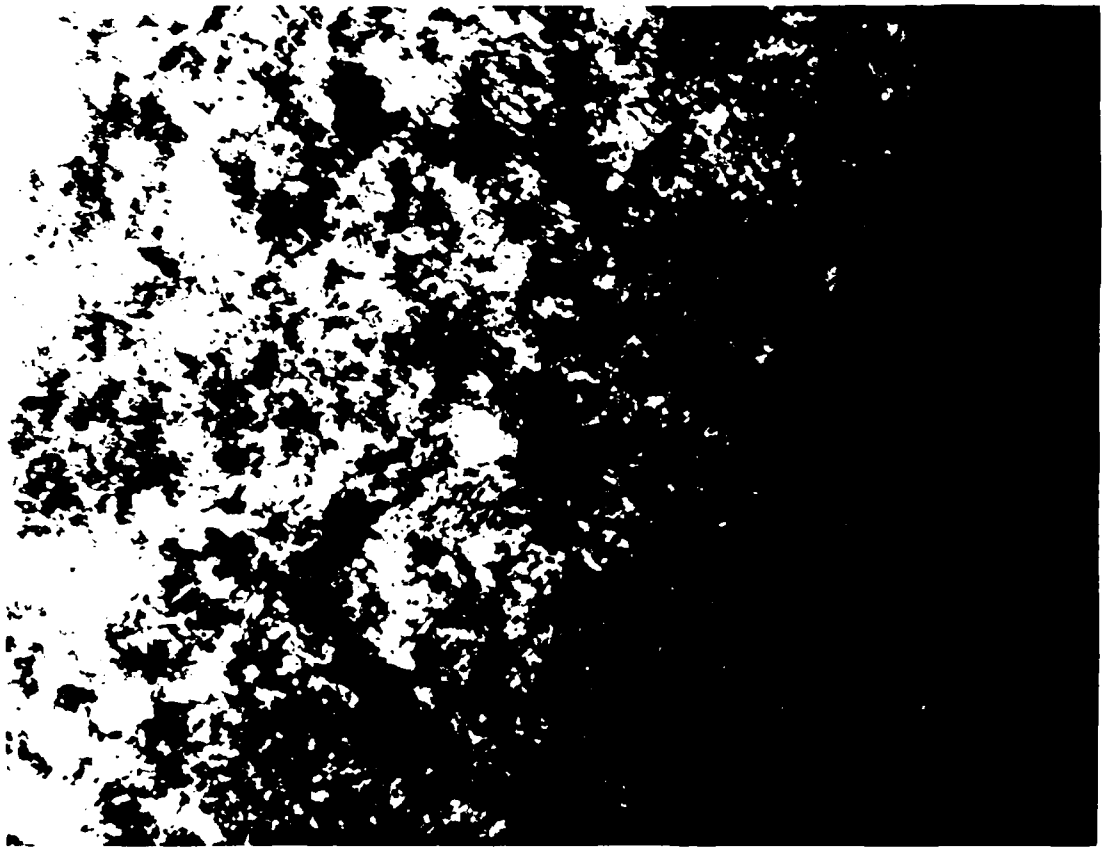

Fig. 11. Transmission electron micrograph, aged for 24 hrs. at 700F (25200X)

Fig. 12. Transmission electron micrograph, aged for 48 hrs. at 1000F (17460X).

Fig. 13. Transmission electron micrograph, duplex aged - 600F/24hr + 1050F/24hr (17460X).

DISTRIBUTION LIST
(One copy only unless otherwise noted)

Commander
Naval Air Systems Command
Attn: Code AIR-5304D6 (2 copies)
Washington, D.C. 20361

AIR-7220 (4 copies)
AIR-5302 (1 copy)
AIR-310A (1 copy)
AIR-310B (1 copy)

Commander Naval Air Development Center
ATTN: M. Thomas, Code 6063 (1 copy)
E. Tankins, Code 6063 (1 copy)
R. Mahorter, Code 6063 (1 copy)
Warminster, PA 18974

Commander
Naval Sea Systems Command
Code 05R
Department of the Navy
Washington, D.C. 20361

Commander
Naval Weapons Center
Code 5516
China Lake, CA 93555

Commander
Naval Surface Weapons Center
Metallurgy Divison - R32 - D. Divecha
White Oak, Silver Spring, Md 20910

Chief of Naval Research
Code ONR 423
ONR 431
800 N. Quincy Street
Arlington, VA 22217

Commander
Naval Air Propulsion Center
Science and Technology Group
ATTN: J. Glatz
Trenton, NJ 08628

ENCLOSURE(3)

Director
Naval Research Laboratory
ATTN: Codes 6300 (1 copy)
6370 (1 copy)
6390 (1 copy)
Washington, D.C. 20375

Air Force Office of Scientific Research
Dept. of the Air Force
Bolling Air Force Base
Washington, D.C. 20322

Air Force Wright Aeronautical
Laboratory
Attn: Code LLM (1 copy)
LLN (1 copy)
Metals Branch, Mfg. Tech Div (1 copy)
Wright-Patterson AFB
Dayton, OH 45433

Army Aviation Systems Command
P.O. Box 209
ATTN: Mr. R. V. Vollmer - AMSAV - FRE
St. Louis, MO 63166

Army Research & Tech. Lab
Applied Technology Lab
DAVDL-ATL-ATS
ATTN: T. Mazza
Ft. Eustis, VA 23604

Army Research Office
Box CM, Duke Station
Attn: Metallurgy & Ceramics Divsion
Durham, NC 27706

Army Matl's & Mech. Research Ctr
Attn: Dr. George Thomas
Watertown, MA 02171

Defense Advanced Research Project Agency
ATTN: Dr. B. A. Wilcox Code 641
1400 Wilson Boulevard
Arlington, VA 22209

NASA
Ames Research Center
Code 240-10
Moffett Field, CA 94035

NASA Jet Propulsion Laboratory
4800 Oak Grove Drive
Pasadena, CA 91103

NASA
Langley Research Ctr
ATTN: R. A. Pride
Langley Station, MS 15d
Hampton, VA 23365

NASA
Marshall Space Flight Ctr
ATTN: R. Schwinghamer
Huntsville, AL 35812

U.S. Department of Energy
Division of Reactor Research & Technology
ATTN: A. Van Echo
Mail Station B-107
Washington, D.C. 20545

National Academy of Sciences
National Materials Advisory Board
2101 Constitution Ave.
ATT: Dr. J. C. Lane
Washington, D.C. 20418

National Science Foundation
1800 G St., N.W.
Washington, D.C. 20550

Battelle Memorial Institute
Mfg. & Design Interaction
ATTN: Dr. Bryan R. Noton
505 King Ave.
Columbus, OH 43201

Metals & Ceramics Info. Cntr.
Battelle, Columbus Laboratories
505 King Avenue
Columbus, OH 43201

Bell Helicopter Co.
Adv. Sys. Programs
ATTN: James Kenna
P.O. Box 482
Ft. Worth, TX 76101

The Boeing Company
Aerospace Division
P.O. Box 3707, M/S 73-43
ATTN: Mr. Rod Boyer
Seattle, WA 98124

Boeing Company
Vertol Division/MS P62-06
ATTN: R. Pinckney
P.O. Box 95006
Philadelphia, PA 19142

EXXON Materials Division
ATTN: Jerry Dixon
P.O. Box 95006
Raleigh, NC 27625

General Dynamics
ATTN: C.F. HERNDON
P.O. Box 748, MS 2830
Ft. Worth, TX 76101

General Dynamics Materials Research
ATTN: W.G. Scheck
P.O. Box 80847, MZ 640-00
San Diego, CA 92138

Grumman Aerospace Corp.
MS AD-12, Materials & Proc. Dept.
ATTN: R. J. Herfzman
South Oyster Bay Road
Bethpage, NY 11714

Grumman Aerospace Corp.
Ad. Mtls & Process Div.
ATTN: Carl Micillo
Dept. 447, Plan 12
Bethpage, NY 11714

Hughes Aircraft Co.
Components & Materials Lab
ATTN: L.B. Keller
Bldg. 6, Main Station, D-134
Culver City, CA 90230

Kaman Aerospace Corp.
Matl's & Process Engineering
ATTN: A.S. Falcone
Old Windsor Road
Bloomfield, CT 06002

LTV Aerospace Corp.
Vought Systems Division
P.O. Box 5907
ATTN: MR. A.B. Hohman, Jr.
Dallas, TX 75222

Lockheed California Co.
Department 70-31 Bldg. 63
ATTN: R. Kaseko/J. Pengra
Burbank, CA 91520

General Electric Company
Corporate Research & Development
ATTN: G. Benn (1 copy)
M.F. Henry (1 copy)
P.O. Box 8
Schenectady, NY 12301

General Electric Company
Aircraft Engine Group
Materials & Processes Technology Laboratories
Cincinnati, OH 45215

General Electric Co.
Aircraft Engine Group
ATTN: J. Hsia
HD A24068
Lynn, MA 01910

Pratt & Whitney Aircraft Division
Florida Research & Development Center
ATTN: M. M. Allen
West Palm Beach, FL 33402

Pratt & Whitney Aircraft Company
United Technologies Company
East Hartford, CT 06108

United Technologies Company
Research Center
400 Main Street
East Hartford, CT 06108

Detroit Diesel Allison Division
General Motors Corporation
Materials Laboratories
Indianapolis, IN 46206

Airesearch Manufacturing Company of Arizona
402 South 36th Street
ATTN: Chief, Materials Engineering Dept.
Dept. 93-03M
P.O. Box 5217
Phoenix, AZ 75010

Lycoming Division
AVCO Corporation
Stratford, CT 06497

Solar
Attn: Dr. A. Metcalfe
2200 Pacific Highway
San Diego, CA 92112

Teledyne CAE
1330 Laskey Road
Toledo, OH 43601

Garrett Turbine Engine Co.
Dept. 93-393/503-4Y
111 S. 34th Street
Phoenix, AZ 85034

Lockheed Missile & Space Co., Inc.
Dept. 86-73
ATTN: F.B. Yarborough
P.O. Box 504, Bldg. 153
Sunnyvale, CA 94088

Martin Marietta Corp.
Denver Division
ATTN: Dr. A. Feldman
P.O. Box 179, MZ 1630
Denver, CO 80201

McDonnell Douglas Aircraft Co.
Mfg. R&D Dept (M31-22)
ATTN: Robert Zwart
3855 Lakewood Blvd.
Long Beach, CA 90846

McDonnell Douglas Corporation
Engineering Division
ATTN: B. B. Leonard
5301 BOLSA/MS A3-248/13-3
Huntington Beach, CA 92347

McDonnell Douglas Research Labs
P.O. Box 516
ATTN: Dr. D. F. Ames
Dr. Charles Whitsett
St. Louis, MO 63166

Northrop Corporation
ATTN: E. Jaffe
d3901 West Broadway Blvd.
Hawthorne, CA 90250

Rockwell International Corp.
ATTN: P.J. Dynes
Science Center
1049 Camino Dos Rios
Thousand Oaks, CA 91360

Sikorsky Aircraft
Mfg. Engineering Dept.
ATTN: J.D. Ray
North Main Street
Stratford, CT 06602

United Technologies Company
Research Center
400 Main Street
East Hartford, CT 06108

END

DTIC

7-86